

## Enhanced thermoelectric properties of $\text{Co}_{1-x-y}\text{Ni}_{x+y}\text{Sb}_{3-x}\text{Sn}_x$ materials

Hong-quan Liu<sup>1)</sup>, Sheng-nan Zhang<sup>2)</sup>, Tie-jun Zhu<sup>2)</sup>, Xin-bing Zhao<sup>2)</sup>, Yi-jie Gu<sup>1)</sup>, and Hong-zhi Cui<sup>1)</sup>

1) College of Materials Science and Engineering, Shandong University of Science and Technology, Qingdao 266510, China

2) State Key Laboratory of Silicon Materials, Development of Materials Science and Engineering, Zhejiang University, Hangzhou 310027, China

(Received: 18 March 2011; revised: 20 June 2011; accepted: 11 July 2011)

**Abstract:**  $\text{Co}_{1-x-y}\text{Ni}_{x+y}\text{Sb}_{3-x}\text{Sn}_x$  polycrystals were fabricated by vacuum melting combined with hot-press sintering. The effect of alloying on the thermoelectric properties of unfilled skutterudite  $\text{Co}_{1-x}\text{Ni}_x\text{Sb}_{3-x}\text{Sn}_x$  was investigated. A leap of electrical conductivity from the  $\text{Co}_{0.93}\text{Ni}_{0.07}\text{Sb}_{2.93}\text{Sn}_{0.07}$  sample to the  $\text{Co}_{0.88}\text{Ni}_{0.12}\text{Sb}_{2.88}\text{Sn}_{0.12}$  sample occurs during the measurement of electrical conductivity, indicating the adjustment of band structure by proper alloying. The results show that alloying enhances the power factor of the materials. On the basis of alloying, the thermoelectric properties of  $\text{Co}_{0.88}\text{Ni}_{0.12}\text{Sb}_{2.88}\text{Sn}_{0.12}$  are improved by Ni-doping. The thermal conductivities of Ni-doping samples have no reduction, but their power factors have obvious enhancement. The power factor of  $\text{Co}_{0.81}\text{Ni}_{0.19}\text{Sb}_{2.88}\text{Sn}_{0.12}$  reaches  $3.0 \text{ mW}\cdot\text{m}^{-1}\cdot\text{K}^{-2}$  by Ni doping. The dimensionless thermoelectric figure of merit reaches 0.55 at 773 K for the unfilled  $\text{Co}_{0.81}\text{Ni}_{0.19}\text{Sb}_{2.88}\text{Sn}_{0.12}$ .

**Keywords:** thermoelectric material; polycrystals; skutterudites; alloying; thermoelectric properties; doping

[This work was financially supported by the National Natural Science Foundation of China (Nos. 50801054 and 51072104) and the Research Award Fund for Outstanding Young Scientists in Shandong Province, China (No. BS2011CL031)]

### 1. Introduction

Thermoelectricity has great potential for applications such as energy conversion of waste heat into electricity and solid state heating and cooling. The efficiency of advanced thermoelectric technology is governed by the dimensionless thermoelectric figure of merit:

$$ZT = \alpha^2 \sigma T / \kappa \quad (1)$$

where  $\alpha$ ,  $\sigma$ ,  $\kappa$ , and  $T$  are the Seebeck coefficient, the electrical conductivity, the thermal conductivity, and the absolute temperature, respectively. Good thermoelectric materials should possess a relatively higher value of power factor ( $\alpha^2 \sigma$ ) and a lower value of thermal conductivity.

$\text{CoSb}_3$ -based skutterudite compounds have attracted much attention as one of the most promising thermoelectric materials. Many efforts have been made to improve the thermoelectric properties of  $\text{CoSb}_3$ , including doping by partial Co-site or Sb-site substitution, filling structure voids,

and multi-site substitution [1-4]. The high properties of many thermoelectric materials such as  $\text{Bi}_2\text{Te}_3/\text{Sb}_2\text{Te}_3$  and  $\text{PbTe}/\text{SnTe}$  are directly related to the formation of solid solutions. Solid solutions of skutterudites offer several important advantages, such as tailoring the energy band gap to the desired operational regime, altering the size of voids, and extending the range of rare-earth ions that can be trapped in the structure. The solid solution of  $\text{CoSb}_3$  may be formed by replacing Sb with Ge and Se, Co with Ni and Fe, or symmetrical replacements can be made on both Co and Sb sites [5]. The multi-channel improving way is being performed by combining multi-site substitution, doping, and multi-filling with nanostructuring at the same time [6]. Reducing the lattice thermal conductivity  $k_L$  is an important factor in obtaining high efficiency energy conversion in all thermoelectric materials [7]. Both the filling and solvothermal technology are important improving methods for reducing thermal conductivity [1, 8]. Filled skutterudites have gained low thermal conductivity and high  $ZT$  values due to the vibration

Corresponding author: Hong-quan Liu E-mail: hq.liu666@yahoo.com.cn

© University of Science and Technology Beijing and Springer-Verlag Berlin Heidelberg 2012

effect and the doping effect from filled elements [1, 9]. The solvothermal synthesis is limited because the low Pauling's electronegativity elements cannot be employed without proper reductants, but the thermoelectric properties of materials (without low Pauling's electronegativity elements) with high power factor can still be improved by the solvothermal synthesis.

In this paper, the thermoelectric properties of  $\text{Co}_{1-x}\text{Ni}_x\text{Sb}_{3-x}\text{Sn}_x$  (no low Pauling's electronegativity elements) were firstly researched in order to improve the thermoelectric properties of  $\text{CoSb}_3$  based materials. On the basis of alloying, the thermoelectric properties of  $\text{Co}_{1-x}\text{Ni}_x\text{Sb}_{3-x}\text{Sn}_x$  were enhanced by further Ni-doping, and the effect of alloying and doping on the thermoelectric properties of  $\text{Co}_{1-x}\text{Ni}_x\text{Sb}_{3-x}\text{Sn}_x$  were discussed.

## 2. Experimental

$\text{Co}_{1-x-y}\text{Ni}_x\text{Sb}_{3-x}\text{Sn}_y$  ( $x = 0.05, 0.07, 0.12, \text{ and } 0.25; y = 0, 0.01, 0.03, 0.05, 0.07, \text{ and } 0.09$ ) compounds were synthesized by reactions between the elements under vacuum in silica tubes. Stoichiometric amounts of Co (99.9%), Ni (99.99%), Sn (99.9%), and Sb (99.99%) shots were sealed in the evacuated quartz ampoules. After melting at 1373 K for 30 h, the ampoules were annealed at 923 K for 5 d. After the heat treatment, the products were grounded into powder and hot pressed at 873 K for 60 min under a pressure of 80 MPa. The samples were analyzed with X-ray diffraction (XRD) on a RigakuD/MAX-2550PC diffractometer using  $\text{Cu K}\alpha$  radiation ( $\lambda = 0.15406 \text{ nm}$ ) in the range of  $2\theta = 10^\circ\text{-}80^\circ$ . The electrical conductivity and Seebeck coefficient were measured at a computer assistant device. The electrical conductivity  $\sigma$  was obtained by a four-probe method. The Seebeck coefficient was calculated with the slope of the thermoelectric power  $\Delta U$  vs. temperature difference  $\Delta T$  from

0 to about 5 K between both ends of the sample. An Agilent 34401A multimeter was used for the measurement of  $\Delta U$ , temperature difference  $\Delta T$ , and temperature. The thermal conductivity  $\kappa$  was measured and calculated by a Netzsch LFA 457 laser flash apparatus.

## 3. Results and discussion

Fig. 1 shows XRD patterns of  $\text{Co}_{1-x}\text{Ni}_x\text{Sb}_{3-x}\text{Sn}_x$  samples with different  $x$  values. All diffraction peaks of the samples are identical to the standard JCPDS card 01-083-0055 of  $\text{CoSb}_3$ , indicating that the dopants are doped into the lattice sites and single phase compounds are obtained.

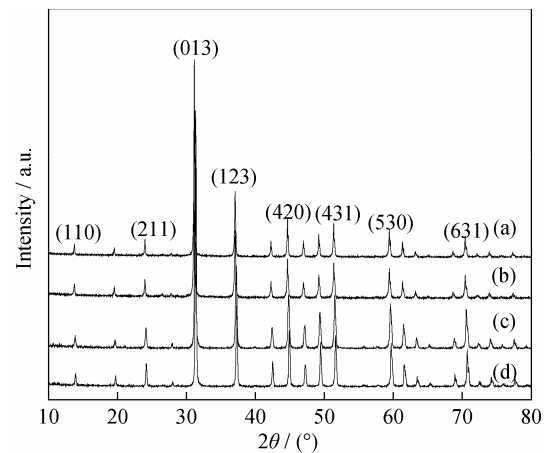


Fig. 1. XRD patterns of  $\text{Co}_{1-x}\text{Ni}_x\text{Sb}_{3-x}\text{Sn}_x$  with different  $x$  values: (a)  $x = 0.05$ ; (b)  $x = 0.07$ ; (c)  $x = 0.12$ ; (d)  $x = 0.25$ .

Fig. 2 shows the temperature dependence of Seebeck coefficients and electrical conductivities for  $\text{Co}_{1-x}\text{Ni}_x\text{Sb}_{3-x}\text{Sn}_x$  samples. There are two Sn position distributions in the  $\text{CoSb}_{3-x}\text{Sn}_x$  system, which was verified by the Mossbauer technology. Due to part Sn as donor impurities, all the samples show n-type conduction with negative Seebeck co-

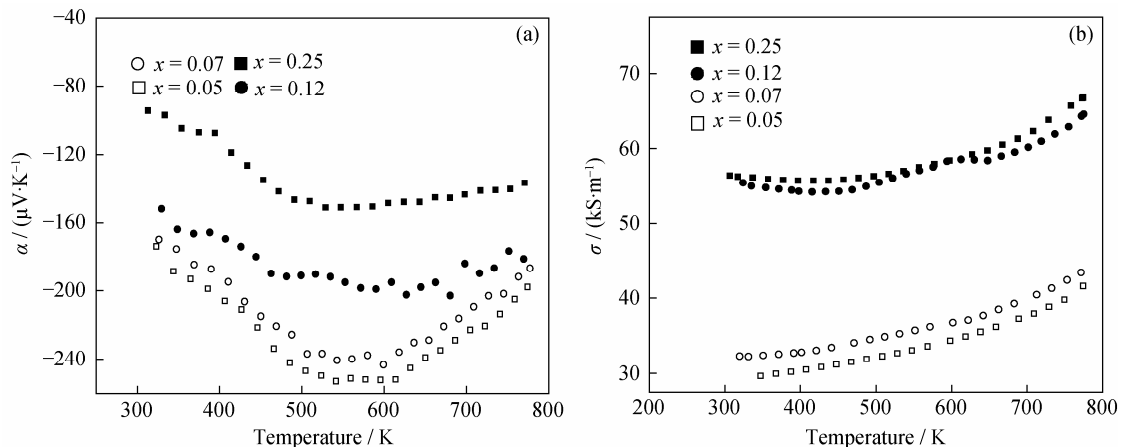


Fig. 2. Seebeck coefficient (a) and electrical conductivity (b) of  $\text{Co}_{1-x}\text{Ni}_x\text{Sb}_{3-x}\text{Sn}_x$ .

efficients. The Seebeck coefficient of the materials firstly increases and then decreases. The maximum value of the Seebeck coefficient is about  $-250 \mu\text{V/K}$  at 600 K for the sample with  $x = 0.05$ .

As a result, the absolute value of Seebeck coefficient decreases with the increase of the  $x$  value, while the electrical conductivity displays a reverse change. This tendency agrees with other reports [10]. A leap of electrical conductivity of  $\text{Co}_{1-x}\text{Ni}_x\text{Sb}_{3-x}\text{Sn}_x$  samples occurs from  $x = 0.07$  to  $x = 0.12$ . The relative densities of all hot-pressed samples varied from 93% to 95%, so the effect of different densities on electrical conductivity may be neglected.

The forbidden band gap  $E_g$  may be estimated according to the following equation [11]:

$$\rho = A \exp\left(\frac{E_g}{k_B T}\right) \quad (2)$$

where  $\rho$  is the electrical resistivity,  $A$  is a constant, and  $k_B$  is the Boltzmann constant.

According to Eq. (2), estimated  $E_g$  are displayed in Table 1. The values of  $E_g$  of the materials changes from 0.048 eV to 0.034 eV as  $x$  increases from 0.07 to 0.12. The estimated  $E_g$  (0.03-0.05 eV) agrees well with the theoretical calculation of about 0.05 eV given by Singh and Pickett [12] and experimental values of 0.035-0.05 eV obtained from various measurements [13-15]. As shown in Table 1, the leap of  $E_g$  from  $x = 0.07$  to  $x = 0.12$  is corresponding to the change of electrical conductivity. Thus, the leap of electrical conductivity comes from the adjustment of band structure in  $\text{Co}_{1-x}\text{Ni}_x\text{Sb}_{3-x}\text{Sn}_x$  by proper alloying. The electrical conductivity of the sample with  $x = 0.25$  does not enhance obviously in comparison with that of the sample with  $x = 0.12$ , which is attributed to the doping limit and a dramatic sup-

pression of carrier mobility from scattering of more point defects [16-17]. The electrical conductivity of the samples ( $x = 0.12, 0.25$ ) reaches about  $6.6 \times 10^4 \text{ S}\cdot\text{m}^{-1}$  at 773 K.

Table 1. Estimated  $E_g$  of  $\text{Co}_{1-x}\text{Ni}_x\text{Sb}_{3-x}\text{Sn}_x$  eV

$x$	0.25	0.12	0.07	0.05
$E_g$	0.038	0.034	0.048	0.050

As shown in Fig. 3, the power factors of  $\text{Co}_{1-x}\text{Ni}_x\text{Sb}_{3-x}\text{Sn}_x$  samples increase with the increase of  $x$  values, but that of the sample with  $x = 0.25$  decreases due to lower Seebeck coefficient. The trend is more obvious at high temperature. The maximum value of the power factor is about  $2.4 \text{ mW}\cdot\text{m}^{-1}\cdot\text{K}^{-2}$  at 623 K for the sample with  $x = 0.12$ , which is higher than that ( $0.66 \text{ mW}\cdot\text{m}^{-1}\cdot\text{K}^{-2}$ ) of  $\text{Co}_{1-x}\text{Fe}_x\text{Ni}_y\text{Sb}_3$  with alloying on the Co site [5]. The proper alloying is in favor of enhancement of the power factor for thermoelectric materials.

On the basis of alloying, the thermoelectric properties of the Ni-doping samples were researched. Fig. 4 shows the See-

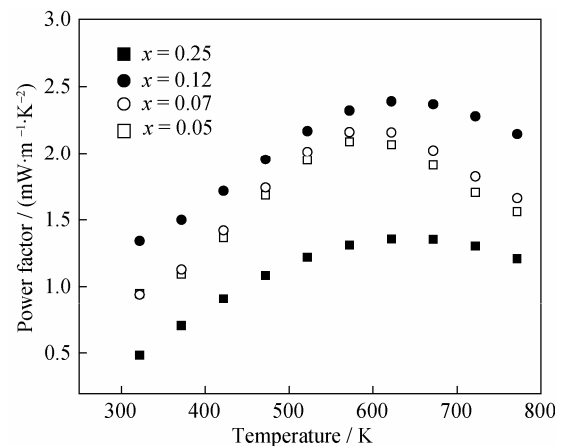


Fig. 3. Power factor of  $\text{Co}_{1-x}\text{Ni}_x\text{Sb}_{3-x}\text{Sn}_x$  with different  $x$  values.

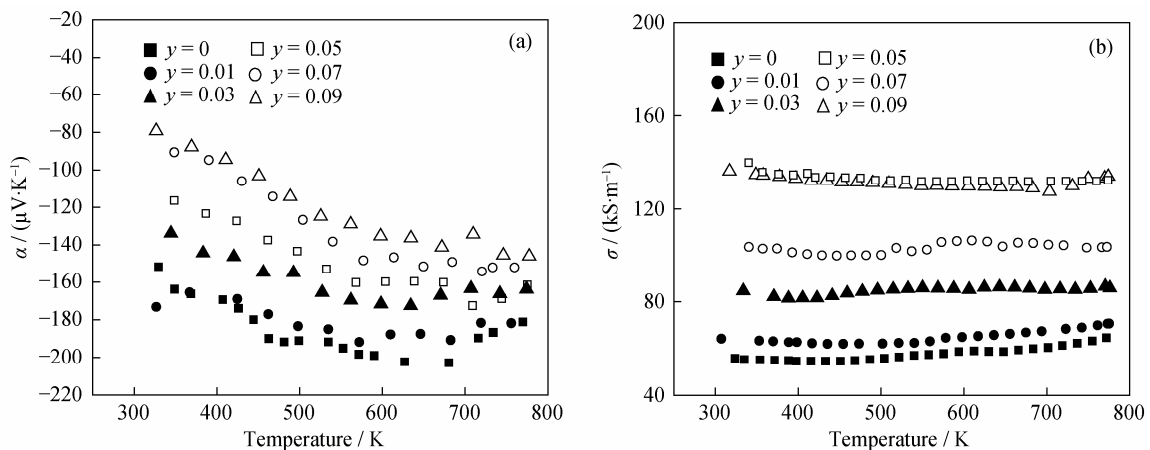
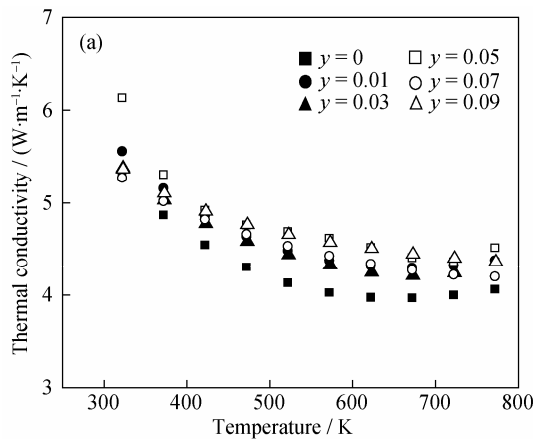


Fig. 4. Seebeck coefficients (a) and electrical conductivities (b) of  $\text{Co}_{0.88-y}\text{Ni}_{0.12+y}\text{Sb}_{2.88}\text{Sn}_{0.12}$  samples.

beck coefficients and electrical conductivities of  $\text{Co}_{0.88-y}\text{Ni}_{0.12+y}\text{Sb}_{2.88}\text{Sn}_{0.12}$  samples with different  $y$  values. The absolute values of Seebeck coefficients of  $\text{Co}_{0.88-y}\text{Ni}_{0.12+y}\text{Sb}_{2.88}\text{Sn}_{0.12}$  samples decrease with the increase of  $y$  values, while their electrical conductivities increase accordingly. This result is attributed to the increase of carrier concentration [18]. The electrical conductivity of the sample with  $y = 0.09$  has no enhancement in comparison with that of the sample with  $y = 0.07$ . The reason may be attributed to the doping limit [16]. Thus, the maximum value of the electrical conductivity is about  $1.32 \times 10^5 \text{ S}\cdot\text{m}^{-1}$  at 623 K for the samples with  $y = 0.07$  and  $0.09$ .

Fig. 5 shows the power factors of  $\text{Co}_{0.88-y}\text{Ni}_{0.12+y}\text{Sb}_{2.88}\text{Sn}_{0.12}$  samples with different Ni-doping contents. Power factors of  $\text{Co}_{0.88-y}\text{Ni}_{0.12+y}\text{Sb}_{2.88}\text{Sn}_{0.12}$  samples are less sensitive to a doping level at low temperature; this is attributed to the non-parabolic nature of energy bands [19]. The power factors of all samples show positive temperature dependence from 323 to 600 K. The power factors of the samples with  $y < 0.05$  display negative temperature dependence from 673 to 773 K, while those of the samples with  $y > 0.05$  still keep positive temperature dependence at above 600 K. The maximum value of the power factor is  $3.0 \text{ mW}\cdot\text{m}^{-1}\cdot\text{K}^{-2}$  at 773 K for the sample with  $y = 0.07$ . The improved power factor can also be attributed to the effect of alloying and Ni-doping [1, 20].

The temperature dependence of thermal conductivities is



shown in Fig. 6(a) for  $\text{Co}_{0.88-y}\text{Ni}_{0.12+y}\text{Sb}_{2.88}\text{Sn}_{0.12}$ . The thermal conductivities of the samples decrease as the temperature increases, while they increase with the increase of  $y$  values due to the increase of carrier's concentration. The thermal conductivity generally includes two parts, one from the charge carriers and another from the lattice vibration. According to the Wiedemann-Franz relation:

$$\frac{\kappa_e}{\sigma T} = L \quad (3)$$

where  $L = 2 \times 10^{-8} \text{ W}\cdot\Omega\cdot\text{K}^{-2}$ ;  $\kappa_e$ ,  $\sigma$ , and  $T$  are the thermal conductivity of the carrier, the electrical conductivity, and the absolute temperature, respectively.

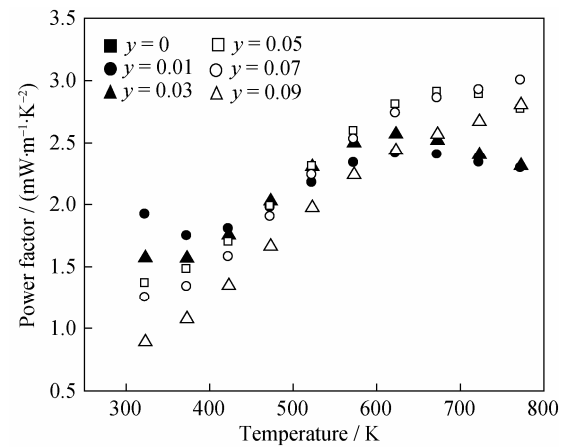


Fig. 5. Power factors of  $\text{Co}_{0.88-y}\text{Ni}_{0.12+y}\text{Sb}_{2.88}\text{Sn}_{0.12}$  samples with different  $y$  values.

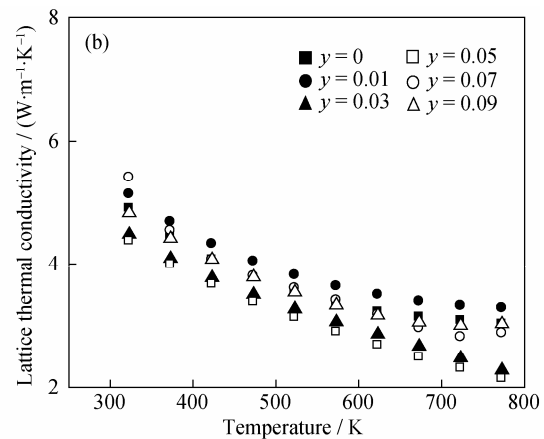


Fig. 6. Thermal conductivity (a) and lattice thermal conductivity (b) of  $\text{Co}_{0.88-y}\text{Ni}_{0.12+y}\text{Sb}_{2.88}\text{Sn}_{0.12}$ .

The value of  $\kappa_c$  can be calculated from Eq. (3). Therefore, the lattice thermal conductivity  $\kappa_L$  can be obtained by  $\kappa_L = \kappa_{\text{total}} - \kappa_c$ . The thermal conductivities from the lattice vibration are shown in Fig. 6(b). As shown in Fig. 6, the thermal conductivities of all samples come mainly from the contribution of the lattice vibration. The solvothermal synthesis

may be applied to reduce the thermal conductivity of  $\text{Co}_{0.88-y}\text{Ni}_{0.12+y}\text{Sb}_{2.88}\text{Sn}_{0.12}$  series further.

The  $ZT$  values of  $\text{Co}_{0.88-y}\text{Ni}_{0.12+y}\text{Sb}_{2.88}\text{Sn}_{0.12}$  samples are shown in Fig. 7. The thermoelectric properties of doped samples are obviously enhanced as the temperature and doped contents increase. The maximum figure of merit  $ZT = 0.55$

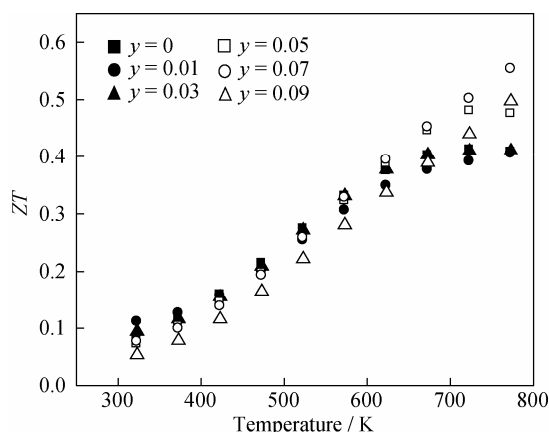


Fig. 7. ZT values of  $\text{Co}_{0.88-y}\text{Ni}_{0.12+y}\text{Sb}_{2.88}\text{Sn}_{0.12}$  samples with different y values.

is obtained for the  $\text{Co}_{0.81}\text{Ni}_{0.19}\text{Sb}_{2.88}\text{Sn}_{0.12}$  sample at 773 K. The nanostructuring (solvothermal synthesis) and filling will improve the thermoelectric properties of  $\text{Co}_{0.81}\text{Ni}_{0.19}\text{Sb}_{2.88}\text{Sn}_{0.12}$  by reducing the thermal conductivity.

#### 4. Conclusion

The alloying was performed by symmetrical replacements on both the Co site and Sb site.  $E_g$  of materials was changed from 0.050 to 0.034 eV by proper alloying. The change results in obvious enhancement of electrical conductivity, while there is only a little losing of Seebeck coefficient. On the basis of alloying, further Ni doping was employed in order to improve the thermo-electric properties of the material. The maximum value of the power factor is 3.0  $\text{mW}\cdot\text{m}^{-1}\cdot\text{K}^{-2}$  at 773 K for the  $\text{Co}_{0.81}\text{Ni}_{0.19}\text{Sb}_{2.88}\text{Sn}_{0.12}$  sample. The high power factor is attributed to the effect of proper alloying and Ni-doping. The maximum figure of merit  $ZT = 0.55$  is obtained for the  $\text{Co}_{0.81}\text{Ni}_{0.19}\text{Sb}_{2.88}\text{Sn}_{0.12}$  sample at 773 K.

#### References

- [1] Q.Y. He, S.J. Hu, X.G. Tang, Y.C. Lan, J. Yang, X.W. Wang, Z.F. Ren, Q. Hao, and G. Chen, The great improvement effect of pores on ZT in  $\text{Co}_{1-x}\text{Ni}_x\text{Sb}_3$  system, *Appl. Phys. Lett.*, 93(2008), art. No.042108.
- [2] W.S. Liu, B.P. Zhang, J.F. Li, H.L. Zhang, and L.D. Zhao, Enhanced thermoelectric properties in  $\text{CoSb}_{3-x}\text{Te}_x$  alloys prepared by mechanical alloying and spark plasma sintering, *J. Appl. Phys.*, 102(2007), art. No.103717.
- [3] X. Shi, H. Kong, C.P. Li, C. Uher, J. Yang, H. Wang, L. Chen, and W. Zhang, Low thermal conductivity and high thermoelectric figure of merit in n-type  $\text{Ba}_x\text{Yb}_y\text{Co}_4\text{Sb}_{12}$  double-filled skutterudites, *Appl. Phys. Lett.*, 92(2008), art. No. 182101.
- [4] X.F. Tang, Q.J. Zhang, L.D. Chen, T. Goto, and T. Hirai, Synthesis and thermoelectric properties of p-type- and n-type-filled skutterudite  $\text{R}_y\text{M}_x\text{Co}_{4-x}\text{Sb}_{12}$  (R:Ce,Ba,Y;M:Fe,Ni), *J. Appl. Phys.*, 97(2005), art. No.093712.
- [5] J.L. Mi, T.J. Zhu, X.B. Zhao, and J. Ma, Thermoelectric properties of skutterudites  $\text{Fe}_x\text{Ni}_y\text{Co}_{1-x-y}\text{Sb}_3$  ( $x=y$ ), *J. Alloys Compd.*, 452(2008), p.225.
- [6] P.N. Alboni, X. Ji, J. He, N. Gothard, and T.M. Tritt, Thermoelectric properties of  $\text{La}_{0.9}\text{CoFe}_3\text{Sb}_{12}\text{-CoSb}_3$  skutterudite nanocomposites, *J. Appl. Phys.*, 103(2008), art. No.113707.
- [7] G.J. Snyder and E.S. Toberer, Complex thermoelectric materials, *Nat. Mater.*, 7(2008), p.105.
- [8] J.L. Mi, T.J. Zhu, X.B. Zhao, and J. Ma, Nanostructuring and thermoelectric properties of bulk skutterudite compound  $\text{CoSb}_3$ , *J. Appl. Phys.*, 101(2007), art. No.054314.
- [9] B.C. Sales, D. Mandrus, B.C. Chakoumakos, V. Keppens, and J.R. Thompson, Electron crystals and phonon glasses filled skutterudite antimonides, *Phys. Rev. B*, 56(1997), p.15081.
- [10] T. He, J.Z. Chen, H.D. Rosenfeld, and M.A. Subramanian, Thermoelectric properties of indium-filled skutterudites, *Chem. Mater.*, 18(2006), p.759.
- [11] W.S. Liu, B.P. Zhang, J.F. Li, and L.D. Zhao, Effects of Sb compensation on microstructure, thermoelectric properties and point defect of  $\text{CoSb}_3$  compound, *J. Phys. D*, 40(2007), p.6784.
- [12] D.J. Singh and W.E. Pickett, Skutterudite antimonides: Quasilinear bands and unusual transport, *Phys. Rev. B*, 50(1994), p.11235.
- [13] D. Mandrus, A. Migliori, T.W. Darling, M.F. Hundley, E.J. Peterson, and J.D. Thompson, Electronic transport in lightly doped  $\text{CoSb}_3$ , *Phys. Rev. B*, 52(1995), p.4926.
- [14] E. Arushanov, M. Respaud, H. Rakoto, J.M. Broto, and T. Caillat, Shubnikov-de Haas oscillations in  $\text{CoSb}_3$  single crystals, *Phys. Rev. B*, 61(2000), p.4672.
- [15] C.S. Lue, Y.T. Lin, and C.N. Kuo, NMR investigation of the skutterudite compound  $\text{CoSb}_3$ , *Phys. Rev. B*, 75(2007), art. No.075113.
- [16] H. Anno, K. Matsubara, Y. Notohara, T. Sakakibara, and H. Tashiro, Effects of doping on the transport properties of  $\text{CoSb}_3$ , *J. Appl. Phys.*, 86(1999), p.3780.
- [17] M. Puyet, A. Dauscher, B. Lenoir, C. Bellouard, C. Stiewe, E. Muller, J. Hejtmanek, and J. Tobola, Influence of Ni on the thermoelectric properties of the partially filled calcium skutterudites  $\text{Ca}_y\text{Co}_{4-x}\text{Ni}_x\text{Sb}_{12}$ , *Phys. Rev. B*, 75(2007), art. No.245110.
- [18] Y.Z. Pei, L.D. Chen, W. Zhang, X. Shi, S.Q. Bai, X.Y. Zhao, Z.G. Mei, and X.Y. Li, Synthesis and thermoelectric properties of  $\text{K}_y\text{Co}_4\text{Sb}_{12}$ , *Appl. Phys. Lett.*, 89(2006), art. No. 221107.
- [19] T. Caillat, A. Borshchevsky, and J.P. Fleurial, Properties of single crystalline semiconducting  $\text{CoSb}_3$ , *J. Appl. Phys.*, 80(1996), p.4442.
- [20] H. Kitagawa, M. Wakatsukia, H. Nagaoka, H. Noguchi, Y. Isoda, and K. Hasezaki, Temperature dependence of thermoelectric properties of Ni-doped  $\text{CoSb}_3$ , *J. Phys. Chem. Solids*, 66(2005), p.1635.